Short Chain Branching Distribution and Thermal Behavior of High Density Polyethylene

YONG-MAN KIM,[1] CHUL-HWAN KIM,[1] JUNG-KI PARK,[1,*] JUNG-WHAN KIM,[2] and TAE-IK MIN[2]

[1]Department of Chemical Engineering, Korea Advanced Institute of Science and Technology, 373-1, Kusung-dong, Yusung-gu, Daejon, 305-701, Korea and [2]Central Research Center, Hanwha Chemical Corporation, 6, Shinsung-dong, Yusung-gu, Daejon, 305-345, Korea

SYNOPSIS

High-density polyethylenes with unimodal and bimodal molecular weight distribution have been fractionated according to crystallizability using preparative temperature rising elution fractionation. The molecular structure and thermal properties of the fractions with their whole polymers have been characterized. The average short chain branching content of the fractions obtained ranged from 0 to 8 branches per 1000 carbon atoms while that of the whole polymers is about 2 branches per 1000 carbon atoms. The bimodal resins have a slightly higher frequency of short chain branch in higher molecular weight species than in those of the unimodal resins. The short chain branching distribution as well as the low molecular weight species in the fractions seem to be important parameters to determine thermal behavior of the fractions. The fractions with the short chain branching content above 3 branches per 1000 carbon atoms showed a significantly different thermal behavior from those with less than 3 branches per 1000 carbon atoms. © 1996 John Wiley & Sons, Inc.

INTRODUCTION

High-density polyethylene (HDPE) is one of the most widely produced polymers in the world. The applications of HDPE resins are very diverse, and various HDPE grades are in use. The diversity of HDPE grades is a result of large variations in molecular structure, such as the average molecular weight, molecular weight distribution (MWD), the type and content of short chain branching (SCB), and short chain branching distribution. The structural characterization of HDPE is thus of considerable interest.

HDPE is the product of ethylene polymerization with density higher than 0.940 g/cm^3 including both ethylene homopolymers and copolymers with higher alpha olefins. HDPE molecules, like linear low-density polyethylene (LLDPE), contain a small number of chain branches which are mainly incorporated by copolymerization of ethylene with alpha olefins, such as 1-butene and 1-hexene. Branching is one of the fundamental structural parameters influencing the chain microstructure, the crystallization behavior, and the morphology of HDPE, as well as the molecular weight.

Recently, considerable effort has been made to investigate the short chain branching of LLDPE.[1-17] There was significant progress in understanding the short chain branching distribution, and its effect on the morphology and thermal properties of LLDPE.[1-17] For HDPE, the majority of molecular characterizations have been more concentrated on the analysis of average molecular weight and molecular weight distribution.[18-27] Only a few studies have been made on the short chain branching distribution of HDPE.[1,16] They reported that HDPE had a bimodal short chain branching distribution composed of a very distinctive sharp peak of low branching together with a broad higher branching tail. They have not shown the dependence of the short chain branching content on the molecular weight.

In this paper, we tried to extend the previous work by investigating the short chain branching distributions of unimodal molecular weight distribution HDPE (unimodal HDPE) and bimodal molecular

* To whom correspondence should be addressed.

Journal of Applied Polymer Science, Vol. 60, 2469-2479 (1996)
 CCC 0021-8995/96/132469-11

weight distribution HDPE (bimodal HDPE). This work will contribute to understanding the characteristic properties of the two kinds of HDPEs.

EXPERIMENTAL

Materials

Four commercial HDPEs, labeled BH, UH, BM, and UM, were used in this study. Some important properties of the materials are listed in Table I. Most properties of the HDPE resins were measured according to ASTM procedures.

Preparative Temperature Rising Elution Fractionation

Fractionation of the HDPE resins was done by preparative temperature rising elution fractionation (preparative TREF). The schematic of the apparatus for preparative TREF used in this study was similar to the preparative TREF system of Wild and Ryle [Fig. 3 of ref. (2)]. The column is loaded with glass beads having a diameter of 2 mm, leaving a total free volume of 400 mL. The HDPE was dissolved in hot xylene at a concentration of 0.015 g/cm^3, stabilized with BHT antioxidant, and then loaded into the column preheated to 132°C. The column was subsequently cooled to room temperature at the rate of 1.2°C/h. During the cooling of the dilute solution the HDPE resin crystallizes onto the glass surface, forming thin layers according to their crystallizability, mostly, short chain branching content, starting from the glass surface. The oil bath was heated at the rate of 10°C/h to the upper temperature of a desired range and was then maintained at this temperature for 30 min. Six hundred milliliters of xylene, preheated to that temperature, was passed upward through the column at a flow rate of 25 mL/min and the eluted solution was collected as a fraction. The column was then heated to the next desired upper temperature and the process repeated. The elution temperature ranges used in this study were as follows: 25 ~ 60°C, 60 ~ 68°C, 68 ~ 76°C, 76 ~ 84°C, 84 ~ 92°C, 92 ~ 100°C, 100 ~ 108°C, and 108 ~ 120°C. The yield of fractions eluted above 120°C was too poor to collect. The fractions were precipitated with acetone, filtered, washed with methanol, and then dried in vacuo at 50°C until constant weight was achieved.

Characterization Methods

Molecular weight and molecular weight distribution of the HDPE resins were determined by gel permeation chromatography (GPC). A Waters 150CV instrument, equipped with two Shodex AT-806MS columns mounted in series, was used. 1,2,4-Trichlorobenzene, containing 0.025 % (w/v) Santanox R antioxidant, was used as the solvent for the GPC system and in the sample preparation. The operating temperature, flow rate, and injection volume were 145°C, 1 mL/min, and 250 μL, respectively. Samples were prepared for injection at a concentration of 0.2 % (w/v) by dissolving at 175°C for 90 min. Characteristics of the columns were calibrated using National Bureau of Standards SRM 1476 polyethylene and narrow polystyrene standards.

Table I Properties of HDPE Resins

		Resin			
Characteristics	Test Method	BH	UH	BM	UM
Melt flow index (g/10 min)	ASTM D 1238				
at 2.16 kg		0.05	0.07	0.32	0.42
21.6 kg		8.5	10.5	27.7	32.6
Density g/cm^3)	ASTM D 1505	0.9535	0.9532	0.9551	0.9535
ESCR, F50 (h)	ASTM D 1693	> 400	130	40	10
Film dart drop impact strength (g)[a]	ASTM D 1709	214	52	—	—
Molecular weight distribution mode	—	Bimodal	Unimodal	Bimodal	Unimodal
Application	—	Film	Film	Blow Molding	Blow Molding

[a] A 20-μm film prepared under the same conditions.

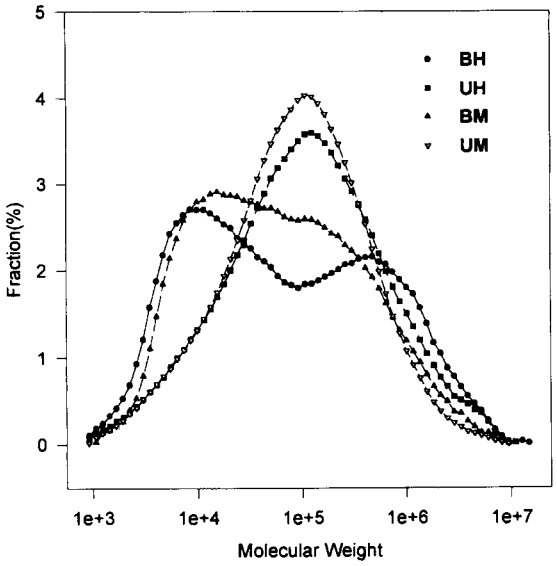

Figure 1 Gel permeation chromatograms of the unfractionated HDPE resins.

The sequence distribution, short chain branching content, and branch type of the HDPE resins were determined by ^{13}C-NMR spectroscopy. The ^{13}C-NMR spectra were recorded on a Bruker AMX 500 NMR spectrometer. Instrument conditions were as follows: pulse angle, 90°; delay time, 9.18 s; acquisition time, 0.82 s; scan number, 2000 ~ 3000; spectra width, 22727.27 Hz; number of data points per spectrum, 16 K; and double precision arithmetic. Sample measurements were taken at 120°C with the inverse gated decoupling method. About 15% (w/v) of the sample solution in a mixed solvent of 80% (v/v) 1,2,4-trichlorobenzene and 20% (v/v) perdeuteriobenzene was measured using a 5-mm tube. The latter solvent was used to provide the internal lock signal. Observed chemical shifts were referenced to an internal hexamethylene disiloxane (HMDS) standard and corrected to tetramethylsilane (TMS) by adding 2.03 ppm.

The crystallization and melting behavior were studied by differential scanning calorimetry (DSC) using the DuPont Thermal Analyst 2000 model. A nitrogen flux of 70 mL/s was sent through the samples during the heating and cooling experiments. Samples ranging in size from 5 to 6 mg were sealed in an aluminum pan and cover for analysis. An indium standard was used to calibrate the temperature scale and enthalpy of melting. First, the sample was melted by raising the temperature to 160°C, kept for 10 min to ensure complete melting and to remove the thermal history. The sample was then cooled to 15°C at the cooling rate of 2°C/min while the crystallization exotherm was recorded. The melting endotherm after crystallization was recorded by heating the sample directly to 160°C at the heating rate of 10°C/min and held for 10 min at that temperature. The sample cell was then submerged into the liquid nitrogen for the rapid crystallization. Finally, the melting endotherm of the quenched sample was obtained with the above procedure.

RESULTS AND DISCUSSION

Molecular Characteristics

Unfractionated HDPE

The molecular weight distributions of the four unfractionated polymers are shown in Figure 1. Resins BH and BM have a bimodal MWD while resins UH and UM have a unimodal MWD.

^{13}C-NMR spectra of the four resins are given in Figure 2. The quantitative ^{13}C-NMR analysis of branching in polyethylene has been a subject of much investigation due to the commercial importance of this material.[28-31] The assignments are well established at present for the products containing less than 10 mol % of the comonomer. The copolymer compositions were determined by ^{13}C-NMR spectroscopy in the conventional manner.[29] It is clear from these spectra that there is no detectable

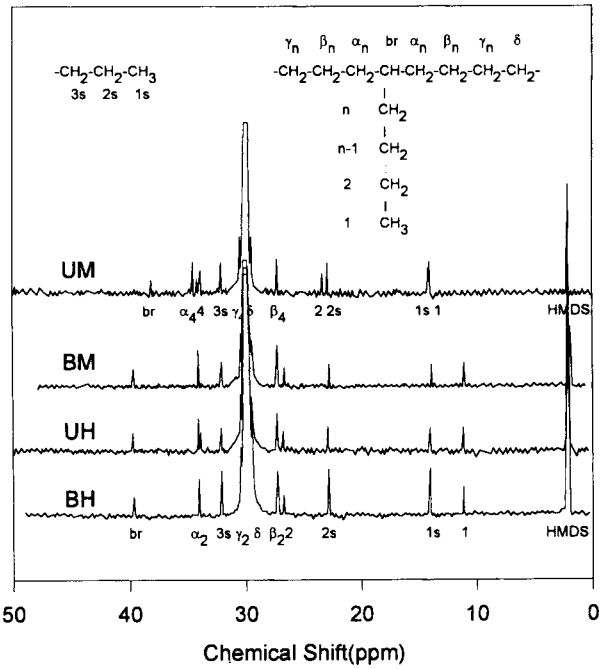

Figure 2 ^{13}C-NMR spectra of the unfractionated HDPE resins.

contiguous comonomer sequence. That is, all of the comonomers are incorporated isolatedly, and the same feature has been reported for medium-density polyethylenes.[29] It is also found from the spectra that short chain branch type of resins BH, UH, and BM is ethyl while that of resin UM is butyl. This concludes that resins BH, UH, and BM are ethylene/1-butene copolymers while resin UM is ethylene/1-hexene copolymer. All the resins show similar average short chain branching content, about 2 branches per 1000 C atoms.

The molecular characteristics, such as average molecular weight, polydispersity, branch type, and average short chain branching content of the HDPE resins are summarized in Table II.

Fractionated HDPE

The separation of a polymer material into its component molecular species constitutes the most important step in any detailed polymer structure study. Through subsequent analysis of the resultant fractions one develops a knowledge of the nature of the complex parent material. The HDPE resins were fractionated into 8 fractions using preparative TREF and the detailed molecular structure of the fractions has been characterized using GPC and ^{13}C-NMR spectroscopy. The elution temperature range, mass percentage, average short chain branching content, number average molecular weight, and polydispersity of the fractions are listed in Table III.

The TREF calibration curve which represents the relation between average elution temperature, defined as the midpoint of the elution temperature interval, and degree of branching for the HDPE resins, is shown in Figure 3. Also, for comparison, included is that of conventional LLDPE (the dotted line) obtained from references.[1,4,8,16] The short chain branching content of the fractions ranged from 0 to 8 branches per 1000 C atoms. As the elution temperature was increased, the short chain branching content was decreased for all the resins. This trend is similar to that of the conventional LLDPE which has some contiguous comonomer sequence. However, the value of the slope of the short chain branching content vs. elution temperature plot is about 4.5 times smaller than that of the conventional LLDPE.[1,4,8,16] The main reason for this apparent discrepancy is the existence of other parameters than comonomer content which also influence the TREF calibration curve. The most important additional parameters seem to be molecular weight, comonomer type and sequence distribution, and experimental conditions. Fractionation by crystallization is known to be independent of molecular weight at molecular weight above 15,000.[33] It has also been reported that when considering the end groups as noncrystallizing defects TREF is independent of molecular weight down to the molecular weight of 1000 although the fractionation temperature is significantly and increasingly molecular weight dependent in the range of low molecular weight less than 10,000. In a separate study, we have examined the TREF calibration curve of the conventional ethylene/1-butene LLDPE polymerized from the Unipol process, which has a density of 0.920 g/cm^3 and a melt index of 1.0. The LLDPE resin contained 4.3 mol % 1-butene and had a monomer dispersity (MD) of 86, which is considerably less than that predicted for a Bernoullian distribution of the same composition. The monomer dispersity is the ratio of the sequence number to the total 1-butene content and represents the tendency of the 1-butene units to form contiguous series.[28,29] The slope of TREF calibration curve of the LLDPE resin was 4.7 times greater than that of the HDPE resins (MD = 100) used in this study. Thus, the discrepancy in TREF calibration curve between the HDPE fractions and the conventional LLDPE fractions can be primarily attributed to the differences in comonomer sequence distribution. It has also been

Table II Molecular Characteristics of HDPE Resins

Characteristics	Resin			
	BH	UH	BM	UM
M_n	12149	21468	15220	22535
M_w	363889	331655	235422	219449
M_w/M_n	30.0	15.5	15.5	9.7
SCB[a] type	Isolated ethyl	Isolated ethyl	Isolated ethyl	Isolated butyl
SCB content, CH_3/1000 C	2.0	1.9	2.1	1.8

[a] Short chain branching.

Table III Molecular Characteristics of Fractions

Sample	Elution Temperature Range (°C)	Weight Fraction	SCB Content (CH_3/1000 C)	M_n	M_w/M_n
BH-1	25–60	0.0101	—	1764	6.3
BH-2	60–68	0.0123	—	2526	12.0
BH-3	68–76	0.0342	5.05	3581	29.6
BH-4	76–84	0.0814	4.7	6467	44.4
BH-5	84–92	0.1551	3.22	9813	33.4
BH-6	92–100	0.4328	1.94	25953	16.2
BH-7	100–108	0.2252	1.45	32087	13.6
BH-8	108–120	0.0489	0	33143	13.3
UH-1	25–60	0.0129	—	2716	6.4
UH-2	60–68	0.0113	—	4086	7.0
UH-3	68–76	0.0188	5.1	4797	7.7
UH-4	76–84	0.0413	4.6	6996	7.2
UH-5	84–92	0.1351	—	12605	6.9
UH-6	92–100	0.4719	1.74	37415	8.3
UH-7	100–108	0.2741	1.57	43089	8.1
UH-8	108–120	0.0346	0	44629	7.7
BM-1	25–60	0.0027	—	1931	31.7
BM-2	60–68	0.0171	—	3788	40.5
BM-3	68–76	0.028	—	4105	36.2
BM-4	76–84	0.0559	5.1	6223	28.6
BM-5	84–92	0.1399	3.11	10652	18.8
BM-6	92–100	0.4603	1.48	29326	9.8
BM-7	100–108	0.2459	1.3	31852	8.9
BM-8	108–120	0.0502	1.2	30748	10.2
UM-1	25–60	0.0087	—	1552	4.4
UM-2	60–68	0.0066	—	2818	7.3
UM-3	68–76	0.0173	—	3523	6.6
UM-4	76–84	0.0452	3.6	6640	7.2
UM-5	84–92	0.1580	2.4	13941	5.8
UM-6	92–100	0.5916	1.43	42698	6.8
UM-7	100–108	0.1561	1.3	39900	7.3
UM-8	108–120	0.0165	0	49161	5.6

noted that the TREF calibration curve for LLDPE depends on the sequence distribution.[32]

Figures 4 and 5 show the molecular weight distributions of the fractions of the higher molecular weight resins BH and UH, respectively. For the fractions eluted below 92°C (> about 3 CH_3/1000 C), it is apparent that the molecular weight of the fractions increases with increasing the elution temperature. For the fractions eluted above 92°C, the molecular weight of the fractions is not significantly varied with increasing elution temperature. It is also found that there are significant differences in molecular weight distributions of the fractions between eluted at the above and below 92°C. The fractions eluted below 92°C have a bimodal MWD irrespective of the MWD mode of the original unfractionated resins. The median value of molecular weight of the higher molecular weight components of the bimodal resin fractions (BH-2, BH-3, BH-4, and BH-5) is about ten times greater than those of the corresponding unimodal resin fractions (UH-2, UH-3, UH-4, and UH-5), as shown in Figures 4 and 5.

From the results of average short chain branching content and molecular weight of the preparative TREF fractions, the dependence of short chain branching content on molecular weight was calculated and given in Figure 6. Short chain branching content of the resins decreases with increasing the molecular weight up to about 50,000 g/mol and then levels off. It is found that there is more short chain branching in high molecular weight species of bimodal resins than in those of the unimodal resins

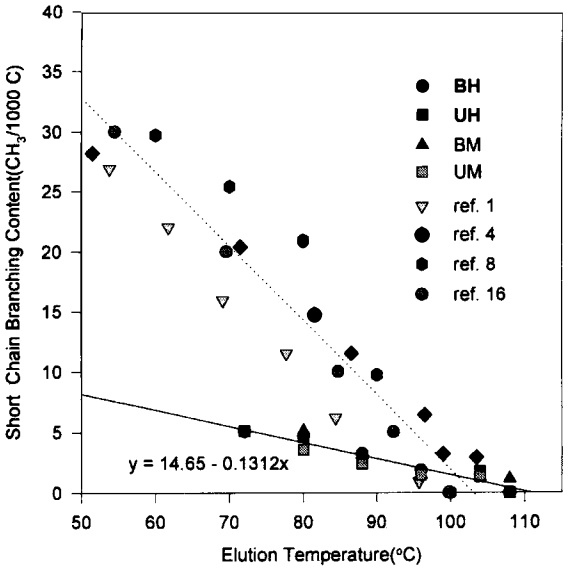

Figure 3 Average short chain branching content of the fractions against the elution temperature.

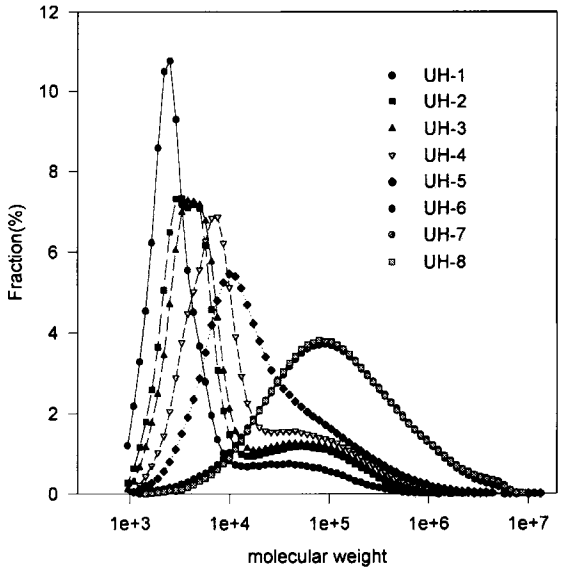

Figure 5 Gel permeation chromatograms of the fractions of the resin UH.

although the differences are small. This would be due to differences in the polymerization process and catalyst used.

Thermal Characteristics

Melting Behavior

The melting behaviors of the fractions and whole polymers were measured by DSC. The thermal history and molecular heterogeneity such as the type, amount, and distribution of branches; molecular weight; and molecular weight distribution determine the morphology and consequently the thermal behavior.

The melting endotherms of resin BH and its fractions which were crystallized at the cooling rate of 2°C/min and by quenching are shown in Figures 7 and 8, respectively. For other resins—UH, BM, UM—and their fractions, the melting thermograms were similar to those of resin BH and its fractions. The melting temperatures (peak and shoulder) and

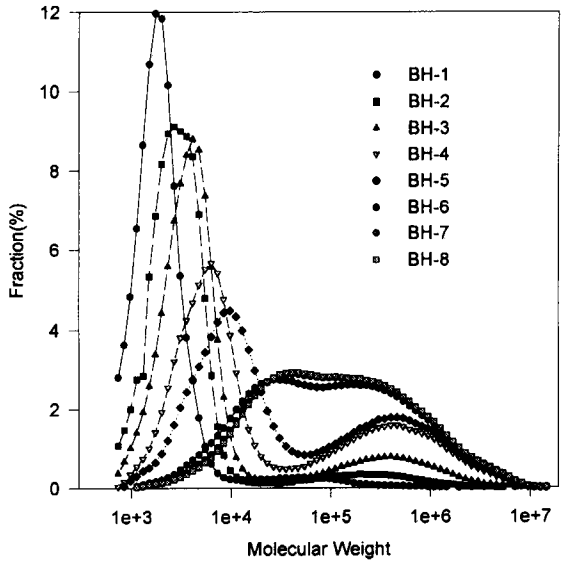

Figure 4 Gel permeation chromatograms of the fractions of the resin BH.

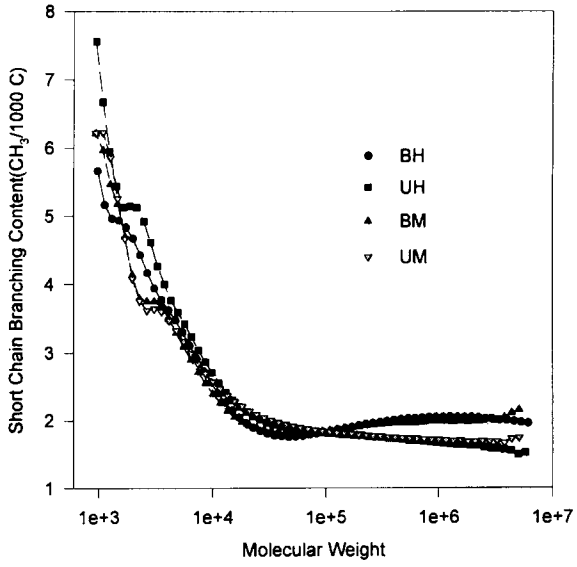

Figure 6 Dependence of short chain branching content on the molecular weight for the HDPE resins.

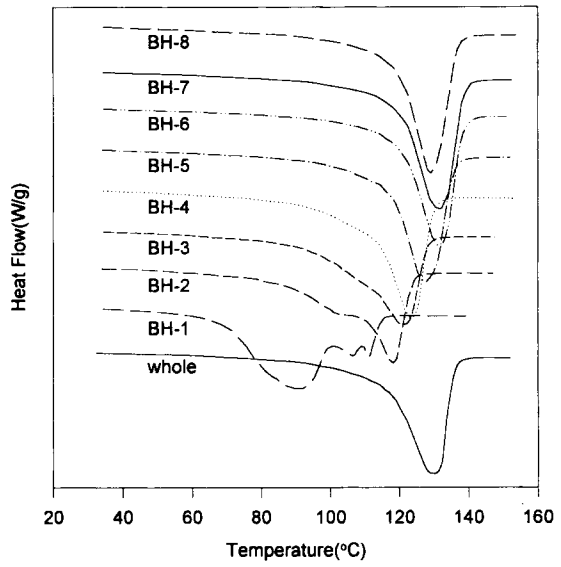

Figure 7 DSC melting endotherms of the unfractionated resin BH and its fractions crystallized at the cooling rate of 2°C/min.

heat of fusion for all the resins and their fractions deduced from the melting endotherms are summarized in Table IV. The melting behavior can reflect their complex morphology. It is generally expected that there is a wide range of lamellae thickness present in the unfractionated HDPE samples, since the branching and molecular weight distribution are broad. The sharper melting peak observed at a higher melting temperature is due to the presence of the thicker lamellae whereas the melting tail of lower temperature is attributed to the thinner lamellae or those having more internal crystallographic imperfection.

For the fractions studied here, the influence of short chain branching content on the thermal behavior needs to be carefully evaluated, since the fractions eluted at the lower temperature contain the low molecular weight tail which can crystallize separately. For the samples crystallized at the cooling rate of 2°C/min., shown in Figure 7, there is a great similarity in variation between the melting endotherm and molecular weight distribution of the fractions. The fractions eluted above 92°C exhibit a single sharp melting peak with broader tail. In contrast, the fractions obtained at the lower elution temperature exhibit a somewhat different pattern of the melting endotherms from the unfractionated polymer. The peak and end melting temperatures of the fractions shift to lower temperatures with increasing average short chain branching content. BH-1 shows a complex melting behavior. This can be attributed to the molecular weight and short chain branching distribution resulting from the wide range of fractionation temperature. For the others, BH-2, BH-3, BH-4, and BH-5, it is noted from the endotherms that there is a distinct secondary melting endotherm developed as a shoulder that appears on the lower temperature side of the melting peak. In the case of the quenched crystallization (Fig. 8), BH-3, BH-4, and BH-5 show a single sharp melting peak with broader tail while BH-2 shows a secondary melting endotherm. It was reported by Mandelkern et al. that during isothermal crystallization of the polydisperse whole polymer only the very low molecular weight species crystallized separately and an extreme upper limit to separate crystallization corresponded to the molecular weight of 7000.[34] Several studies have shown that for rapid crystallization or quenching, cocrystallization of the species occurs, when the molecular weight of the species is higher than 2000.[35,36] For slow cooling, thermodynamic equilibrium of the mixture is generally sustained throughout the crystallization process, whereas in the case of rapid crystallization the diffusion of the molecules is impeded in the melt such that segregation is not feasible. Since these fractions (BH-2, BH-3, BH-4, and BH-5) contain some portion of low molecular weight species with molecular weight less than 10,000, it is necessary to consider whether the melting behavior of these fractions is affected by the presence of the low molecular weight species or not. For this purpose, the hexane extraction was carried out on the fraction BH-2, and the melting behavior and molecular weight of the extract and

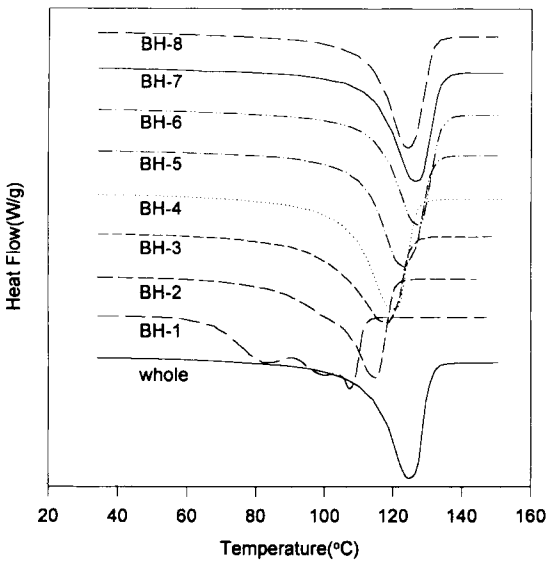

Figure 8 DSC melting endotherms of the unfractionated resin BH and its fractions quenched in liquid nitrogen.

Table IV DSC Melting Characteristics of Fractions and Whole Polymers

	Slowly Cooled			Quenched		
	Melting Temperature (°C)			Melting Temperature (°C)		
Sample	Peak	Shoulder	Heat of Fusion (J/g)	Peak	Shoulder	Heat of Fusion (J/g)
BH-1	90.0	—	221.8	107.6	—	193.9
BH-2	118.0	102.2	191.5	114.4	98.9	177.1
BH-3	121.2	105.8	198.7	117.5	—	176.6
BH-4	123.5	107.4	207.8	119.8	—	184.4
BH-5	127.4	109.4	213.4	122.8	—	186.9
BH-6	131.8	—	210.5	127.5	—	173.6
BH-7	131.6	—	213.4	126.4	—	178.3
BH-8	129.2	—	211.6	124.5	—	174.6
BH (whole)	129.5	—	209.3	124.6	—	180.0
UH-1	91.9	—	193.2	105.7	—	171.8
UH-2	114.1	102.2	201.7	109.6	—	179.1
UH-3	117.4	105.8	214.0	113.2	—	200.1
UH-4	121.6	—	198.9	118.2	—	195.4
UH-5	125.7	—	227.1	121.9	—	190.4
UH-6	131.7	—	203.0	127.5	—	169.1
UH-7	132.4	—	207.9	128.1	—	177.1
UH-8	131.9	—	202.2	125.8	—	170.0
UH (whole)	128.9	—	207.8	123.9	—	173.9
BM-1	108.7	—	178.7	107.6	—	161.3
BM-2	116.7	102.3	175.8	113.5	98.4	153.3
BM-3	118.2	106.2	185.3	114.6	—	162.2
BM-4	122.8	107.2	193.7	118.0	—	183.7
BM-5	128.7	109.8	223.9	124.2	—	193.7
BM-6	131.9	—	223.9	128.8	—	178.3
BM-7	131.6	—	218.2	129.7	—	178.5
BM-8	131.4	—	220.2	127.3	—	177.8
BM (whole)	129.6	—	211.0	124.7	—	181.7
UM-1	91.8	—	223.1	105.8	—	187.7
UM-2	115.6	102.7	217.9	112.4	100.7	192.9
UM-3	117.0	107.7	221.4	112.5	—	194.8
UM-4	121.2	—	230.8	116.6	—	202.6
UM-5	125.0	—	231.8	121.4	—	194.5
UM-6	131.2	—	205.6	127.8	—	181.8
UM-7	131.6	—	206.1	127.1	—	170.2
UM-8	130.0	—	205.5	124.8	—	172.2
UM (whole)	128.8	—	215.6	123.4	—	177.8

residue were analyzed. In Figure 9, the melting endotherms of the hexane extract and residue of BH-2 are compared with that of BH-2. The peak melting temperatures of the extract and residue are almost the same as the secondary and peak melting temperature of BH-2, respectively. The GPC chromatograms of the fraction BH-2 and its hexane extract and residue are shown in Figure 10. It is clear from the results shown in Figures 9 and 10 that the secondary melting endotherm of the fractions is also caused by the presence of the low molecular weight species. For the fractions of unimodal HDPE, UH-4 and UH-5 did not show the apparent secondary melting, as shown in Table IV. This difference between BH and UH resins seems to be due to the molecular weight differences in higher molecular weight component of the fractions (Figs. 4 and 5). The same trend was also ob-

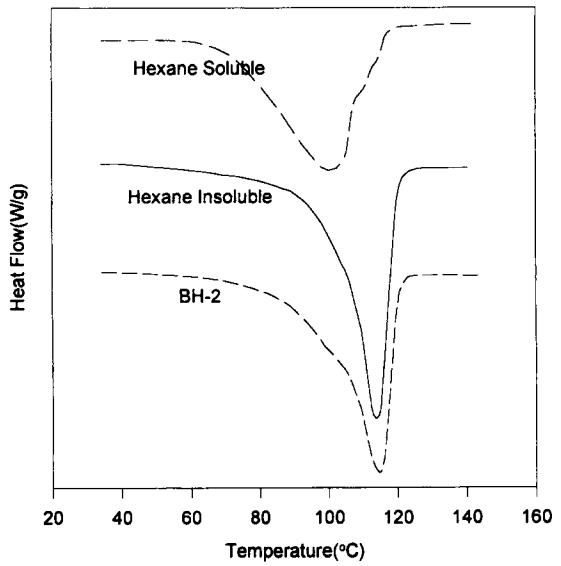

Figure 9 DSC melting endotherms of the fraction BH-2 and its hexane extract and residue crystallized by quenching.

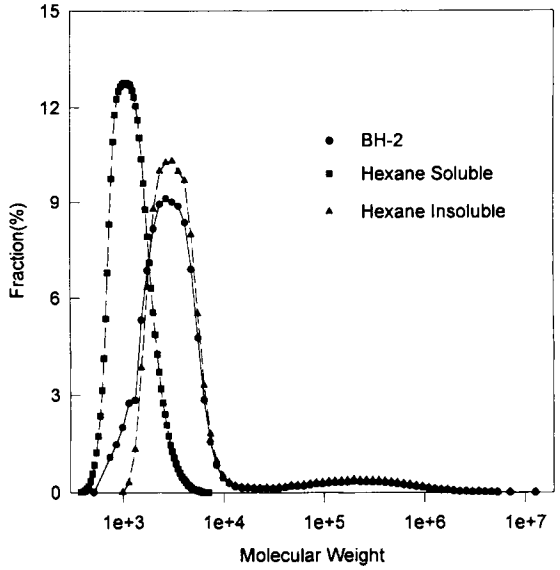

Figure 10 Gel permeation chromatograms of the fraction BH-2 and its hexane extract and residue.

served for medium molecular weight resins BM and UM.

In Figure 11, the peak melting temperatures of all the quenched fractions are plotted with respect to short chain branching content. For comparative and reference purposes, two reference curves, obtained from references,[7,37] are given. The dotted line represents the results for the hydrogenated polybutadine that possesses a random sequence distribution. The dashed line is for the conventional compositional ethylene/1-butene copolymer fractions. Similar effect of short chain branching content on the peak melting temperature was observed for the bimodal and unimodal HDPE resins. The peak melting temperature of the fractions increases gradually with decreasing the short chain branching content, i.e., increasing elution temperature, at the higher ranges (>3CH_3/1000 C) but levels off at the lower short chain branching contents. It is noted that the variation of melting temperature with short chain branching content for the fractions studied here is almost the same as for the hydrogenated polybutadiens, but it is significantly different from the compositional ethylene/1-butene copolymer fractions. The lower melting temperature of the HDPE fractions than the compositional LLDPE fractions at the same branch concentration can be primarily attributed to small differences in the sequence distribution parameters, χ, in the well known relation.[7,37-39]

$$1/T_m - 1/T_{mo} = -(R/\Delta H_u)\ln \chi$$

Here T_m is the melting temperature characterized by χ, T_{mo} is the melting temperature of the corresponding homopolymer, and ΔH_u is the enthalpy of fusion per repeating unit. It has also been demonstrated by Hosoda[17] that the slope of a melting temperature vs. short chain branching content plot decreases with increasing the degree of comonomer blockiness for LLDPEs.

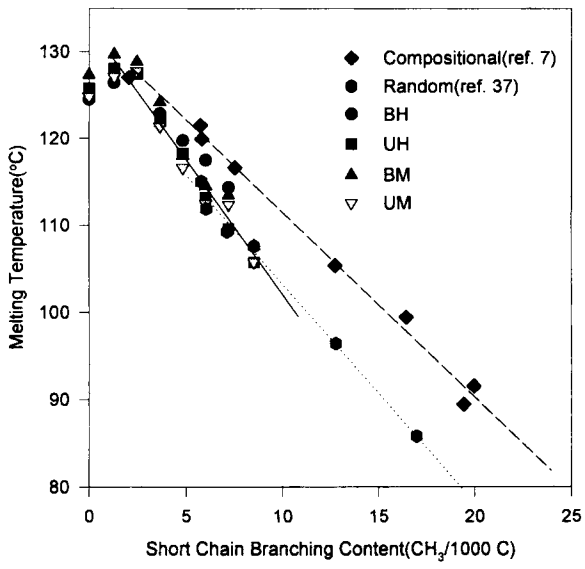

Figure 11 Melting temperature against the short chain branching content for the fractions quenched in liquid nitrogen.

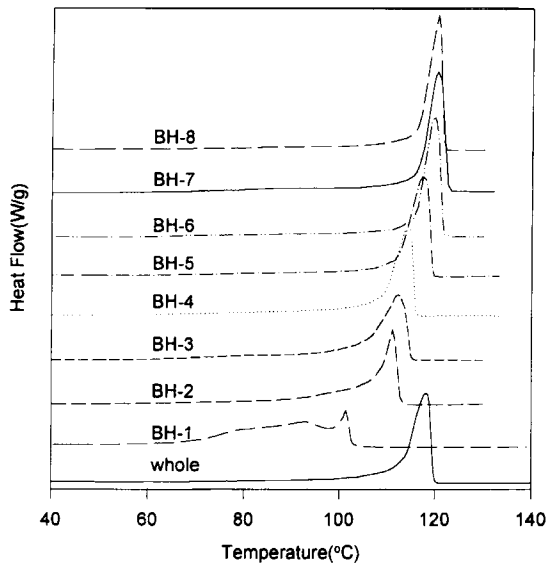

Figure 12 DSC crystallization exotherms of the resin BH and its fractions crystallized at the cooling rate of 2°C/min.

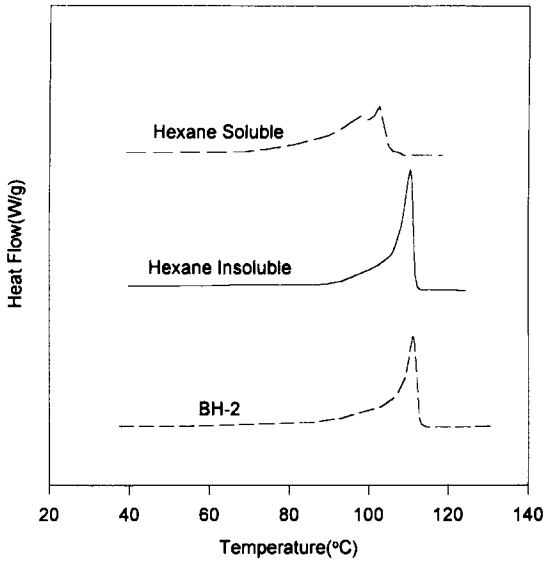

Figure 14 DSC crystallization exotherms of the fraction BH-2 and its hexane extract and residue crystallized at the cooling rate of 2°C/min.

Crystallization Behavior

The crystallization exotherms of resin BH and its fractions crystallized at the cooling rate of 2°C/min. are shown in Figure 12. For other resins—UH, BM, and UM—and their fractions, the crystallization exotherms were very similar to those of resin BH and its fractions.

The unfractionated resin BH exhibits a sharp exotherm with a broad tail due to the heterogeneity resulting from polydispersity as well as short chain branching distribution. The crystallization exotherms of the fractions eluted above 92°C show a similar pattern to that of the unfractionated resin. The fractions eluted above 92°C have narrower width at half height and less noticeable tail than the whole polymer due to narrower short chain branching distribution. However, for the fractions eluted below 92°C, there is a remarkable exotherm tail especially for BH-1, BH-2, and BH-3, and it becomes more conspicuous with decreasing the elution temperature. The crystallization temperature of the fractions increases with decreasing the short chain branching content and levels off, as shown in Figure 13. The effect of the low molecular weight species on the crystallization exotherm tail of the fractions has been investigated in the same manner as is in the melting behavior of them. The crystallization exotherms of the fraction BH-2 and its hexane extract and residue are shown in Figure 14. As was previously discussed in detail, it is clear from these results that the reason for the decrease in the peak crystallization temperature is the effect of increase in the short chain branching content. The remarkable tails are seemed to be due to the presence of low molecular weight species.

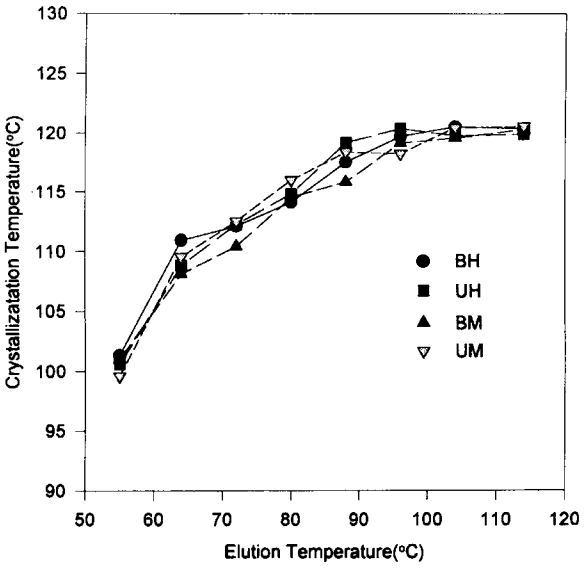

Figure 13 DSC crystallization temperatures of the fractions crystallized at the cooling rate of 2°C/min.

Support of this work by Hanwha Chemical Corporation is gratefully acknowledged.

REFERENCES

1. L. Wild, T. R. Ryle, D. C. Knobeloch, and I. R. Peat, *J. Polym. Sci. Polym. Phys. Ed.*, **20,** 441 (1982).
2. L. Wild, *Adv. Polym. Sci.*, **98,** 1 (1990).
3. L. Wild, *TRIP*, **1,** 50 (1993).
4. F. Defoor, G. Groeninckx, P. Schouterden, and B. Van der Heijden, *Polymer*, **33,** 3878 (1992).
5. F. Defoor, G. Groeninckx, H. Reynaers, P. Schouterden, and B. Van der Heijden, *Macromolecules*, **26,** 2575 (1993).
6. H. Springer, A. Hengse, and G. Hinrichsen, *J. Appl. Polym. Sci.*, **40,** 2173 (1990).
7. R. G. Alamo and L. Mandelkern, *Macromolecules*, **22,** 1273 (1989).
8. E. Karbashewski, L. Kale, A. Rudin, W. J. Tchir, D. G. Cook, and J. O. Pronovost, *J. Appl. Polym. Sci.*, **44,** 425 (1992).
9. B. Monrabal, *J. Appl. Polym. Sci.*, **52,** 491 (1994).
10. R. G. Alamo and L. Mandelkern, *Macromolecules*, **24,** 6480 (1991).
11. D. L. Wilfong and G. W. Knight, *J. Polym. Sci. Polym. Phys. Ed.*, **28,** 861 (1990).
12. Xiao-Qi Zhou and J. N. Hay, *Eur. Polym. J.*, **29,** 291 (1993).
13. T. Usami, Y. Gotoh, and S. Takayama, *Macromolecules*, **19,** 2722 (1986).
14. D. Van der Sanden and R. W. Halle, *TAPPI 1992, Polymers, Laminations & Coatings Conference Proceedings*, Lake Buena Vista, 103 (1992).
15. D. R. Burfield and N. Kashiwa, *Makromol. Chem.*, **186,** 2657 (1985).
16. F. M. Mirabella, Jr. and E. A. Ford, *J. Polym. Sci. Polym. Phys. Ed.*, **25,** 777 (1987).
17. S. Hosoda, *Polym. J.*, **20,** 383 (1988).
18. V. B. F. Mathot, in *New Advances in Polyolefins*, T. C. Chung Eds., Plenum Press, New York, 1993, p. 121.
19. J. Fatou and L. Mandelkern, *J. Phys. Chem.*, **69,** 417 (1965).
20. E. Ergoz, J. G. Fatou, and L. Mandelkern, *Macromolecules*, **5,** 147 (1972).
21. J. Maxfield and L. Mandelkern, *Macromolecules*, **10,** 1141 (1977).
22. I. G. Voight-Martin, E. W. Fischer, and L. Mandelkern, *J. Polym. Sci. Polym. Phys. Ed.*, **18,** 2347 (1980).
23. I. G. Voight-Martin and L. Mandelkern, *J. Polym. Sci. Polym. Phys. Ed.*, **19,** 1769 (1981).
24. I. G. Voight-Martin and L. Mandelkern, *J. Polym. Sci. Polym. Phys. Ed.*, **22,** 1901 (1984).
25. I. G. Voight-Martin, R. Alamo, and L. Mandelkern, *J. Polym. Sci. Polym. Phys. Ed.*, **24,** 1283 (1986).
26. V. B. F. Mathot and M. F. J. Pijpers, *Polym. Bull.*, **11,** 297 (1984).
27. L. Mandelkern, A. Prasad, R. G. Alamo, and G. M. Stack, *Macromolecules*, **23,** 3696 (1990).
28. E. T. Hsieh and J. C. Randall, *Macromolecules*, **15,** 1402 (1982).
29. J. C. Randall, *J. Macromol. Sci.-Rev. Macromol. Chem. Phys.*, **C29,** 201 (1989).
30. T. Usami and S. Takayama, *Macromolecules*, **17,** 1756 (1984).
31. M. De Pooter, P. B. Smith, K. K. Dohrer, K. F. Bennett, M. D. Meadows, C. G. Smith, H. P. Schouwenaars, and R. A. Geerards, *J. Appl. Polym. Sci.*, **42,** 399 (1991).
32. E. Karbashewski, A. Rudin, L. Kale, and W. J. Tchir, *Polym. Eng. Sci.*, **33,** 1370 (1993).
33. J. G. Fatou, in *Encyclopedia of Polymer Science and Engineering*, 2nd ed., H. F. Mark and J. L. Kroschwitz, Eds., New York, 1989, Suppl. Vol., p. 231.
34. R. H. Glaser and L. Mandelkern, *J. Polym. Sci. Polym. Phys. Ed.*, **26,** 221 (1988).
35. P. Smith and R. St. J. Manley, *Macromolecules*, **12,** 483 (1979).
36. P. H. C. Shu, D. J. Burchell, and S. L. Hsu, *J. Polym. Sci. Polym. Phys. Ed.*, **18,** 1421 (1980).
37. R. Alamo, R. Domszy, and L. Mandelkern, *J. Phys. Chem.*, **88,** 6587 (1984).
38. P. J. Flory, *J. Chem. Phys.*, **17,** 223 (1949).
39. P. J. Flory, *Trans. Faraday Soc.*, **51,** 848 (1955).

Received May 1, 1995
Accepted November 19, 1995